Electronic structure and related properties of silver

G. Fuster,* J. M. Tyler, N. E. Brener, and J. Callaway
Department of Physics and Astronomy, Louisiana State University, Baton Rouge, Louisiana 70803-4001

D. Bagayoko
Department of Physics, Southern University, Baton Rouge, Louisiana 70813
(Received 15 May 1990)

We report a nonrelativistic self-consistent, all-electron, local-density-functional calculation of the electronic structure of silver. The linear combination of Gaussian orbitals method is used. We present our results for the band structure, density of states, Fermi surface, Compton profiles, and optical conductivity. Our results are compared with experiments and with other calculations where possible.

I. INTRODUCTION

The electronic structure of silver has been studied theoretically by many authors using a variety of methods. References 1–13 list some calculations dating from 1969 onwards. (See Ref. 1 for references to earlier work.) However, much of the previous work discusses only the energy levels, or these in conjunction with the density of states and the Fermi surface. Much less consideration has been given to related quantities which we wish to emphasize in the present work: the charge and momentum densities and the optical conductivity. Although we have not been able to locate experimental results for the charge form factors for comparison, we do find rather good agreement with experiment in regard to both the Compton profile and the optical conductivity. The latter is particularly interesting since the agreement remains rather good for photon energies up to about 15 eV. In addition, we have been able to identify a flat band at a high excitation energy which has recently been observed in an inverse-photoemission experiment.

In the remainder of this Introduction we review some of the essential features of the band structure of silver and discuss some of the calculations which have previously been reported. Our calculation, which includes all electrons and is fully self-consistent but nonrelativistic, is based on the local-density approximation and was performed using the linear combination of Gaussian orbitals (LCGO) method.[14] It is described in Sec. II. The calculated band structure and density of states are presented in Sec. III. Our results are compared with other calculations and with experiments. The Fermi surface is described in Sec. IV. Our results for the Compton profile and the charge form factors are given in Sec. V, and the optical conductivity is described in Sec. VI. Conclusions are summarized in Sec. VII.

Up to roughly 5 eV above the Fermi energy, the band structure of silver can be described in terms of a broad, nearly-free-electron-like, s-p band which overlaps and hybridizes with a relatively narrow d-band complex (in silver the d-band width is about 3.5 eV). In a rough, general, way the band structures of all the noble metals and the $3d$, $4d$, and $5d$ transition metals are similar in this respect. However, the Fermi level falls in the d-band complex for the transition metals while in the noble metals, the d bands are full. Silver is distinguished by the fact that the top of the d-band complex is about twice as far below the Fermi energy as it is in copper (the bottom of the d band in silver is only 0.6 eV above the lowest s state). In comparison with gold, the position of the d bands in silver relative to E_F is lower by a larger factor, about 2.5. No optical absorption due to interband transitions is possible in silver for visible light. This fact produces the characteristic differences in the visual appearance of silver as compared with copper and gold.

Although the d bands are occupied, the Fermi surfaces of the noble metals are not just spheres, but contain features which result from the buried d-band complex. These are the "necks" around the L points (center of hexagonal faces) of the Brillouin zone. As described by Jepsen *et al.*,[9] hybridization of the d bands with the free-electron band generally raises the energy of the portion of the latter which is above the d bands, and thus also raises the Fermi energy. However, such hybridization is forbidden by symmetry for the $L_{2'}$ state, which is therefore lower in energy than might otherwise be expected, and is an occupied state in contrast with expectations based on a purely free-electron picture. Since the d band is further below the Fermi energy in silver than in either copper or gold, the influence of hybridization on the bands near the Fermi energy is smaller in silver than in the others, and consequently the radius of the L neck is also smaller.

We now turn to a brief description of a few of the many previous calculations. Christensen[1] calculated the band structure of silver using both nonrelativistic and relativistic forms of the augmented-plane-wave method. His calculations were not self-consistent: the crystal potential was constructed from a superposition of atomic (Dirac-Slater) charge densities, and the exchange was included in the $X\alpha$ approximation with $\alpha=1$. This exchange approximation does not yield good results when the calculation is carried to self-consistency. Christensen

also calculated the density of states and the interband contribution to the imaginary part of the dielectric function, $\epsilon_2(\omega)$. This calculation was done in an approximation in which matrix elements are treated as constant and yields only the joint density of states.

Moruzzi *et al.*[3] made a fully self-consistent but nonrelativistic calculation of the band structure of silver using the Green's-function method with a local exchange-correlation potential. This work, which is summarized briefly in the only published report, gives the band structure, the density of states, cohesive properties, and the charge density within the "muffin-tin" sphere.

Jepsen *et al.*[9] used the linear augmented-plane-wave (LAPW) method to perform a self-consistent calculation of the electronic bands, density of states, and Fermi surface of silver. The potentials were constructed using the local approximation to the linear muffin tin orbitals method. Relativistic band shifts were included, but no spin-orbit effects were considered. No further properties are reported. MacDonald *et al.*[10] used the spin-orbit-linearized augmented-plane-wave (SO-LAPW) method with a relativistic exchange-correlation potential to perform a self-consistent calculation of the electronic structure of silver. Non-muffin-tin corrections were included. They report results for a few band energies, the density of states, and the Fermi surface. Eckardt *et al.*[11] calculated the band structure, Fermi surface, density of states, and charge density for silver. Their calculation is performed self-consistently, by using the linear rigorous cellular method. An $X\alpha$ exchange potential was used with $\alpha=0.82$.

II. METHOD OF CALCULATION

Our calculations were performed using the LCGO method, as implemented in the program BNDPKG.[14] The method is based on the Kohn-Sham local-density approximation of Hohenberg-Kohn density-functional theory. It has been applied in the past to calculate the electronic structure of various metals,[15–24] and most recently for the cubic metals of the 4*d* transition series (Nb, Mo, Rh, and Pd).[21–24] No shape approximations (muffin tin) are made to the crystal potential. The method of calculation is described in detail in Ref. 14. It has an advantage that the wave functions in the solid are obtained in a form which is convenient for the calculation of other properties, such as the Compton profile and the optical conductivity. Spin-orbit coupling and other relativistic effect are not included.

Some specific aspects of the present calculation are as follows: We use the Gaussian basis set of Ref. 25, including 16 *s*-type, 12 *p*-type, and 8 *d*-type functions, plus an *f*-type orbital of exponent 0.8. A local exchange-correlation potential of the von Barth–Hedin type was used, in the form parametrized by Rajagopal *et al.*[26] The iterations leading to self-consistency were performed using 89 points within a $\frac{1}{48}$ irreducible wedge of the Brillouin zone. The final bands were calculated at 505 points. The density of states was calculated using the Lehmann-Taut analytical tetrahedron method.[27–30] The procedures to calculate the Comptron profile[31,32] and the optical conductivity[18,19,33] have been described elsewhere. A zero-temperature lattice constant of 7.7218 a.u. was estimated from measured thermal-expansion coefficients.

III. BAND STRUCTURE AND DENSITY OF STATES

Our calculated energy bands are shown in Fig. 1 up to an energy of about 30 eV above the Fermi energy. Some characteristic energy differences relating mostly to the occupied bands are given in Table I. This table also contains results from some other calculations for comparison. Several photoemission experiments have been reported,[34–39] particularly with reference states along the Δ and Λ axes. Some values from these measurements are also given in Table I.

Some of the energies with which we wish to compare our results are given in the literature with reference to the double group, i.e., include spin-orbit coupling. Since our results do not include this, we have removed (approximately) the spin-orbit splitting by forming a weighted average of the energies.

The general features of the band structure are in accord with the discussion given above in the Introduction to this paper. We wish to comment on some aspects of the results as given in Table I.

First, we note the generally excellent agreement between the present results and those of Moruzzi *et al.*[3] These are both fully self-consistent but nonrelativistic calculations employing (slightly different) local exchange-correlation potentials. The calculations were made by quite different numerical methods: LCGO in the present case, and the Green's-function method in Ref. 3. The agreement supports a belief that a satisfactory standard of numerical precision has been achieved for this system.

Second, we note that the present calculation, as well those of Refs. 3 and 9 which employ local exchange-correlation potentials, place the *d* bands too close to the Fermi energy (by roughly 0.7 eV in the present case) in comparison with experiments. The agreement between theoretical and experimental results for energy differences within the *d*-band complex is much better than for the position of the complex. In particular, our calculations do not appear to overestimate the *d*-band width appreciably, as was found to be the case in nickel.[40] That local-density calculations tend to place the *d* bands in the noble metals too high in energy (too close to E_F) was pointed out by Jepsen *et al.*,[9] and occurs even when relativistic corrections are included in the exchange-correlation potential.[10] In contrast, Ref. 11 reports values for the *d*-band position in better agreement with experiment, but this seems to have been achieved by employing an unphysically large value of α in the $X\alpha$ exchange potential.

The question of the adequacy of standard local-density band calculations in metals at energies well above E_F is of particular interest because no theorem exists to guarantee that single-particle energy differences are good approximations to actual excitation energies. The calculation of the optical conductivity, for which the results will be

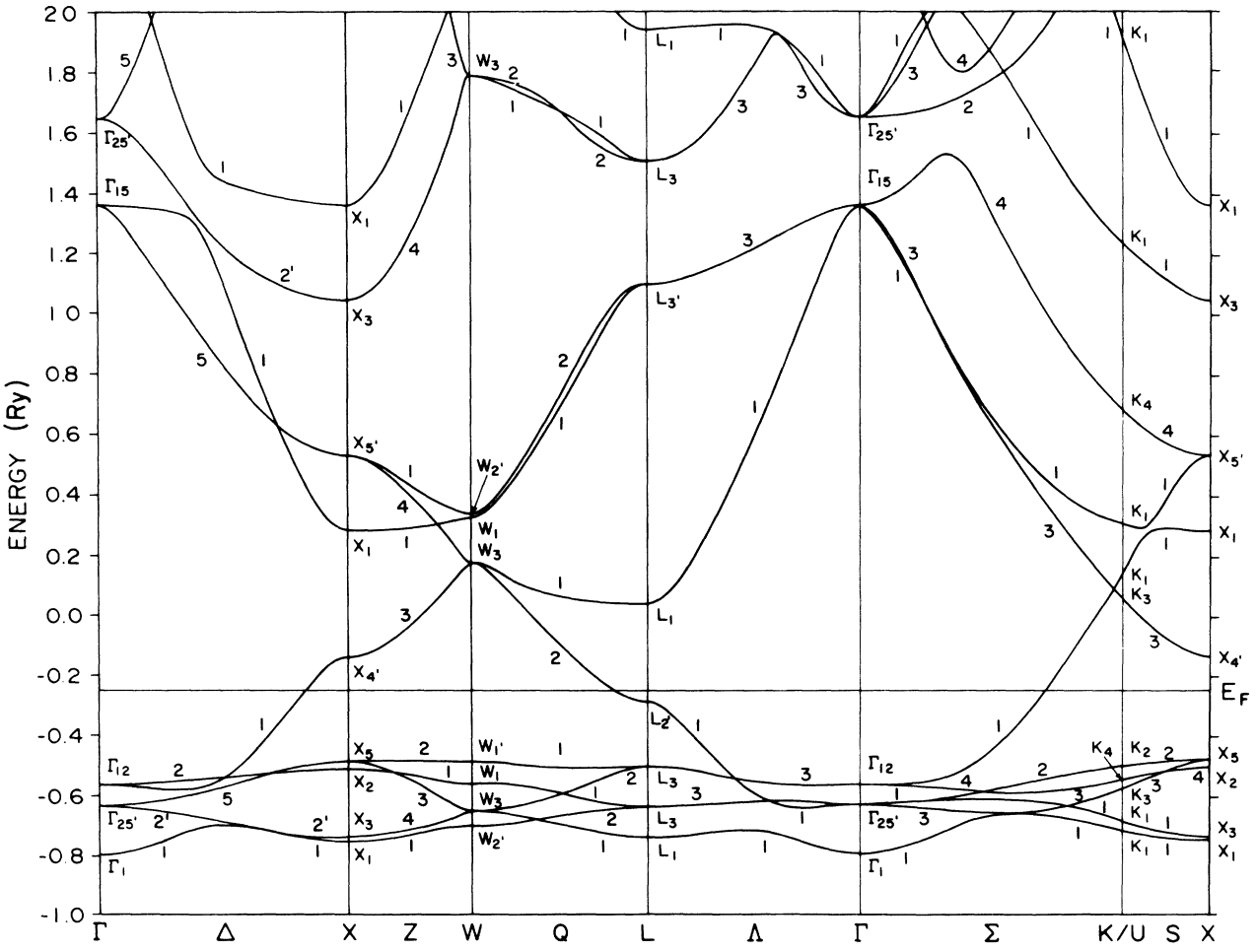

FIG. 1. Energy bands of fcc silver along some lines of symmetry.

TABLE I. Comparison of selected theoretical and experimental results for some energy level differences. All values are in Ry. Spin-orbit splittings have been removed where relevant by making a degeneracy weighted average.

	Theory				Experiment		
	Present	(Ref. 11)	(Ref. 9)	(Ref. 3)	(Ref. 35)	(Ref. 34)	(Ref. 53)
$E_{\Gamma_{12}}-E_{\Gamma_{25'}}$	0.068	0.072	0.074	0.068	0.080	0.082	
$E_{X_{4'}}-E_{X_5}$	0.345	0.453	0.319	0.363			
$E_{X_5}-E_{X_2}$	0.025	0.026	0.021	0.019	0.028		0.022
$E_{X_5}-E_{X_3}$	0.256	0.215	0.263	0.242	0.246		0.228
$E_{X_5}-E_{X_1}$	0.267	0.229	0.287	0.257	0.250		0.253
$E_{L_1(2)}-E_{L_{2'}}$	0.331	0.255	0.322				
$E_{L_{2'}}-E_{L_3(2)}$	0.214	0.301	0.168	0.219			
$E_{L_3(2)}-E_{L_3(1)}$	0.135	0.114	0.139	0.128	0.159	0.134	
$E_{L_3(2)}-E_{L_1(1)}$	0.236	0.192	0.255	0.222		0.216	
$E_F-E_{\Gamma_{12}}$	0.315	0.345	0.271	0.310	0.364	0.364	
$E_F-E_{\Gamma_1}$	0.546	0.530	0.582	0.533			
$E_F-E_{X_5}$	0.235	0.286	0.194	0.238	0.292		0.287
$E_F-E_{L_3(2)}$	0.253	0.303	0.211	0.254	0.302	0.308	

presented subsequently, is related to this issue. Here we note comparison with a recent angle-resolved inverse-photoemission measurement,[39] which reported the existence of a rather flat band about 17 eV above the Fermi energy. Such a feature is not present in a nearly-free-electron picture. We have identified a nearly flat band running from the midpoint of the Δ axis to the L point, parallel to a (011) axis (not shown in Fig. 1). The width of this band is, for $k_x = \frac{1}{2}(2\pi/a)$, less than 0.03 Ry. In our calculations, the band is located at an energy of about 18.5 eV above E_F. We believe this band is that observed in Ref. 39. The error in the calculated energy is roughly 10% (or less), which indicates that the band results are reasonably satisfactory for fairly large excitations.

The present calculation has neglected relativistic effects. Spin-orbit coupling leads to a splitting of degeneracies at symmetry points of the zone (estimated as 0.019 Ry for $\Gamma_{25'}$ according to Ref. 10), but does not have a large effect away from symmetry points. Other effects (the Darwin term and the mass-velocity correction) are included in a second order "scalar-relativistic" calculation. The principal result of these effects is to lower the energies of states of "s" symmetry. Thus, our results for the energy differences such as $E_F - E_{\Gamma_1}, E_{L_3(2)} - E_{L_1}$, and $E_{X_5} - E_{X_1}$ might be expected to be underestimated. This effect seems to be present in the comparison between our results and the scalar relativistic calculation of Ref. 9, but it is apparently obscured in the comparison with the fully relativistic calculation of Ref. 11 by the use (in the latter paper) of an overly large exchange potential which should lower the energies of d states more than s states. (It is probably this effect which leads to rather good results for the d-band position relative to E_F in the results of Ref. 11.)

The density of states is shown in Fig. 2. As expected, all complicated structures related to the d bands lie well below the Fermi surface. The value of the density of states at the Fermi level is $D(E_F) = 3.659$ atom^{-1} Ry^{-1}. This value agrees well with the results of other calculations. A comparison is given in Table II. Using our value of $D(E_F)$, we obtain a value of 0.634 mJ mol^{-1} deg^{-2} for the Sommerfeld coefficient of specific heat γ. The corresponding experimental value of Martin[41] is 0.640 mJ mol^{-1} deg^{-2}. Hence, we find an enhancement factor of only 1.01. This is rather small, compared to the value estimated by Grimvall[42] which is 1.10.

TABLE II. Density of states (in units of atom^{-1} Ry^{-1}) at the Fermi level.

	$D(E_f)$
Present	3.659
Ref. 3	3.673
Ref. 9	3.72
Ref. 10	3.575
Ref. 11	3.524

IV. FERMI SURFACE

The Fermi surface of silver has been studied experimentally using the de Haas–van Alphen effect by Halse[43] and more recently by Coleridge and Templeton.[44] In Fig. 3, we show the cross section of the Fermi surface across some planes of symmetry. The free-electron sphere is indicated for comparison. The radii of the Fermi surface in the [100] and [110] directions are presented in Table III, together with the radius of the neck at point L, along the Q direction. Our results are compared with the experimental values of Coleridge and Templeton,[44] and with the calculated values of Eckardt *et al.*,[11] and MacDonald *et al.*[10] The agreement of our values with the experiment is reasonably good, except in the case of the neck radius. Our value is 25% higher than the measured value. This is to be expected, since the radius of the neck is very sensitive to the position of $L_{2'}$ with respect to the Fermi energy. Although we do not have an experimental value for this energy, it is probable that our result for the energy of $L_{2'}$ is too low compared with the Fermi energy because errors in the position of the d bands tend to raise E_F while $L_{2'}$ is not affected. Our calculated radii for the Fermi surface in other directions are in good agreement with experiment.

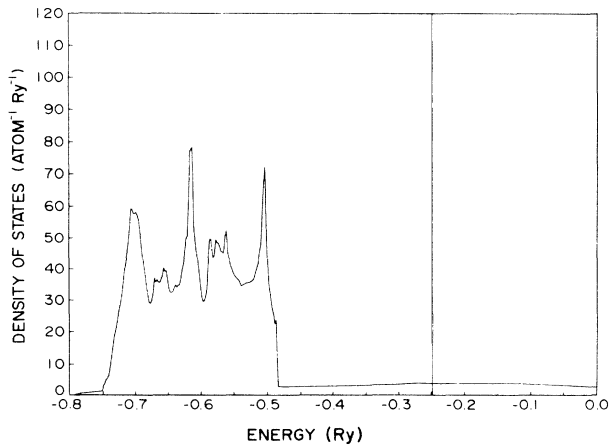

FIG. 2. Density of states of silver.

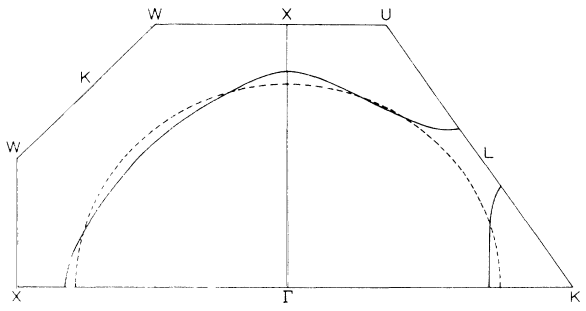

FIG. 3. Fermi-surface cross sections in the (100) and (110) planes.

TABLE III. Fermi-surface radii (in units of $2\pi/a$).

Direction	Experiment Ref. 44	Theory Present	Theory Ref. 11	Theory Ref. 10
[100]	0.819	0.821	0.808	0.827
[110]	0.753	0.741	0.758	0.758
Neck (along the Q direction)	0.107	0.137	0.055	0.104

V. COMPTON PROFILES AND CHARGE FORM FACTORS

We have calculated the Compton profiles of fcc silver by using our self-consistent bands and wave functions. The procedure is explained in detail elsewhere.[31,32] The core contributions were not included in our calculations, since a Hartree-Fock calculation of the contribution of core electrons is already available in the literature.[45] We are not aware of previous calculations of the Compton profile of silver from self-consistent energy bands (non-self-consistent results have been reported[46]). In Table IV, we present our results for the quantity $J_{\hat{k}}(q)$, (as defined in Ref. 31), in the [100], [110], and [111] directions, together with the angular average. In order to compare our results with the experimental results of Sharma *et al.*,[47] the core contributions to the Compton profile from Ref. 45 were added to the valence part. The results are shown in Fig. 4. The agreement is reasonably good. Figure 5 shows our results for the anisotropy of the profile. We are not aware of any experimental measurements of these anisotropic effects.

Our calculated charge form factors are listed in Table V for both the free atom and the solid. The bulk value is usually smaller than the corresponding free atomic value

TABLE IV. Compton profiles for silver (valence contributions only).

Q (Ry)	[100]	[110]	[111]	Average
0.00	3.532	3.578	3.500	3.545
0.05	3.527	3.564	3.499	3.537
0.10	3.512	3.536	3.497	3.519
0.15	3.487	3.481	3.500	3.488
0.20	3.454	3.432	3.482	3.452
0.25	3.414	3.381	3.444	3.407
0.30	3.369	3.323	3.387	3.352
0.35	3.330	3.255	3.291	3.285
0.40	3.255	3.175	3.183	3.200
0.45	3.152	3.080	3.068	3.097
0.50	2.992	2.969	2.947	2.970
0.55	2.847	2.847	2.830	2.843
0.60	2.725	2.698	2.725	2.713
0.65	2.621	2.594	2.637	2.613
0.70	2.553	2.542	2.567	2.552
0.75	2.500	2.491	2.514	2.500
0.80	2.446	2.442	2.459	2.447
0.85	2.389	2.394	2.401	2.394
0.90	2.328	2.349	2.339	2.341
0.95	2.264	2.304	2.275	2.285
1.00	2.206	2.258	2.211	2.231
1.10	2.087	2.157	2.089	2.120
1.20	1.968	2.036	1.973	2.000
1.30	1.832	1.887	1.847	1.861
1.40	1.680	1.727	1.715	1.711
1.50	1.551	1.570	1.575	1.566
1.60	1.430	1.417	1.439	1.426
1.70	1.304	1.257	1.311	1.284
1.80	1.179	1.100	1.183	1.144
1.90	1.070	1.009	1.059	1.039
2.00	0.974	0.931	0.947	0.947
2.20	0.770	0.793	0.777	0.782
2.40	0.622	0.651	0.625	0.636
2.60	0.496	0.515	0.499	0.505
2.80	0.395	0.400	0.393	0.397
3.00	0.303	0.290	0.303	0.297
3.50	0.156	0.157	0.155	0.156
4.00	0.080	0.082	0.079	0.081
5.00	0.028	0.027	0.028	0.028

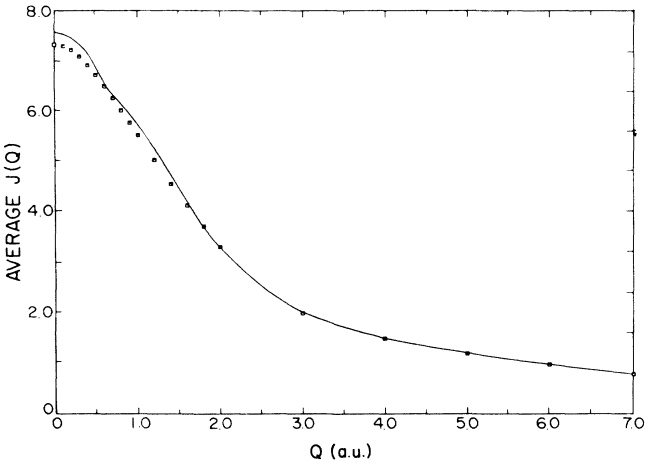

FIG. 4. Spherical average Compton profile, solid line, present calculation; squares, experimental results from Ref. 47.

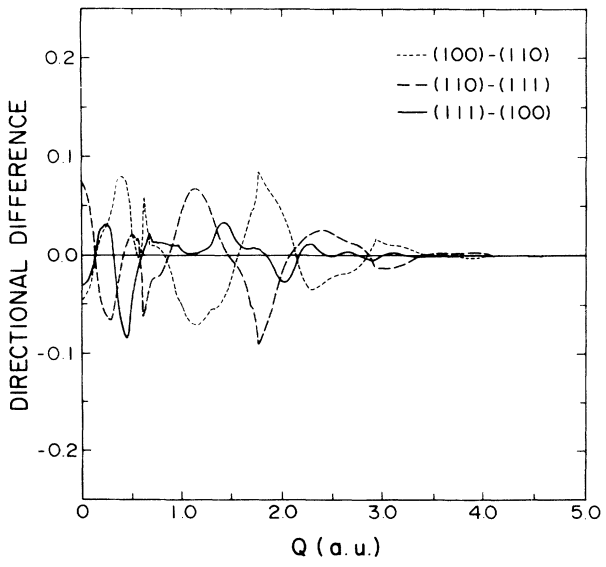

FIG. 5. Anisotropy of calculated Compton profile.

TABLE V. Charge form factors of silver. The angular anisotropies are the ratios of form factors for reciprocal lattice vectors of the same magnitude.

h	k	l	Atom	Solid
0	0	0	47	47
1	1	1	38.188	37.213
2	0	0	36.295	35.305
2	2	0	30.894	30.037
3	1	1	28.201	27.443
2	2	2	27.466	26.737
4	0	0	25.082	24.475
3	3	1	23.717	23.181
4	2	0	23.321	22.816
4	2	2	21.956	21.551
3	3	3	21.109	20.772
5	1	1	21.109	20.786
4	4	0	19.928	19.707
5	3	1	19.320	19.163
4	4	2	19.131	18.989
6	0	0	19.131	19.005
		Angular anisotropies		
	(511)-(333)			1.000 65
	(600)-(442)			1.000 87

because the electron density in the solid is smoother. No experimental results were found in the literature.

VI. OPTICAL CONDUCTIVITY

There are many experimental studies on the optical properties of silver (see Ref. 48 and references therein). These experiments provide a rather full picture of the behavior of the imaginary part of the dielectric constant $\epsilon_2(\omega)$ in a wide range of photon energies, up to 10^4 eV. Christensen[1] performed a theoretical calculation of the optical conductivity in the interband transition region, by using the constant matrix element approximation.

We have calculated the frequency-dependent interband optical conductivity, by integration over the Brillouin zone. The formula and method of calculation are described in detail elsewhere.[18,19,33] The momentum matrix elements are evaluated analytically, which is straightfor-

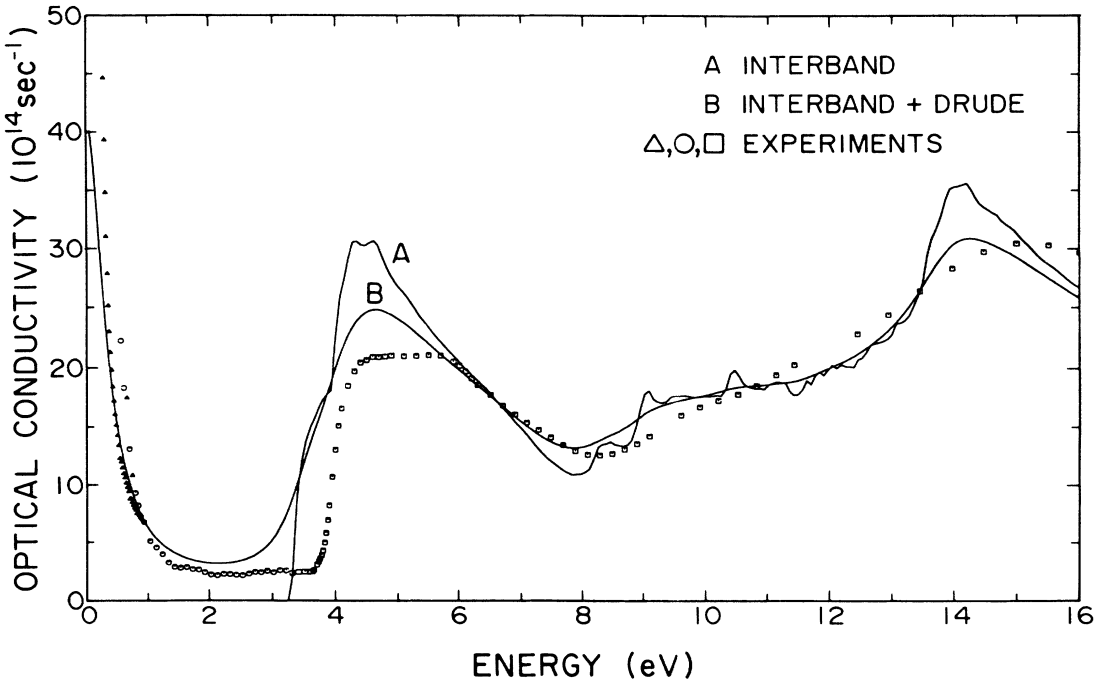

FIG. 6. Optical conductivity of silver. Curve A, interband; curve B, interband plus Drude; ○, Ref. 49; △, Ref. 50; □, Ref. 51.

ward, with the use of the Gaussian orbitals. The results are presented in Fig. 6 (solid curves). Experimental results[49–51] are also shown for comparison (symbols). Curve A represents the calculated interband contribution to the optical conductivity. Curve B represents the interband plus the Drude optical conductivity. The Drude parameters ($\sigma_0 = 5.41 \times 10^{17}$ sec^{-1} and $\tau^1 = 3.65 \times 10^{-14}$ sec.), were obtained from Bennett and Bennett.[52]

In a general way, all major features up to 15 eV are reproduced reasonably well by our calculation. There are differences between theory and experiment. It was observed earlier that density-functional calculations place the d band too close to the Fermi energy by about 0.7 eV. This is clearly apparent in Fig. 6. However, the broad peak around 5 eV, a small shoulder at 10 eV, and a major peak at 15 eV agree with the data, and the overall comparison of the magnitude of the conductivity is satisfactory.

VII. CONCLUSIONS

We have calculated the electronic structure of silver on the basis of local-density-functional theory using the LCGO method for band structures. Relativistic effects were neglected. Energy bands were obtained for energies up to about 30 eV above the Fermi energy. The density of states, the Fermi surface, charge from factors, the Compton profile, and the optical conductivity have been obtained. In general, agreement with experiment is rather good, and this is particularly true for the optical conductivity. The implication is that local-density-functional calculations of energy levels and wave functions are not greatly in error up to photon energies of 15 eV. In addition, we have located a flat band, observed in inverse-photoemission measurements, at about 17 eV above E_F. Our error in regard to the position of this band is 10% (or less) of the excitation energy. At lower energies we find, in agreement with previous studies, that energies of the occupied d bands are too close to the Fermi energy by about 0.7 eV. This seems to be primarily a problem of the local-density approximation, since relativistic calculations by other authors show similar behavior.

ACKNOWLEDGMENTS

We wish to thank Dr. Han Chen for helpful discussions. This work was supported in part by the State of Louisiana Board of Regents under Contract No. LEQSF(1986–1989)A-RD-15 and by the National Science Foundation under Grant No. DMR-88-10249.

*Permanent address: Facultad de Ciencia, Universidad Federico Santa Maria, Casilla Postal 110-V, Valparaíso, Chile.

[1]N. E. Christensen, Phys. Status Solidi B **31**, 635 (1969); **54**, 551 (1972).
[2]A. B. Chen and B. Segall, Phys. Rev. B **12**, 600 (1985).
[3]V. L. Moruzzi, J. F. Janak, and A. R. Williams, *Calculated Electronic Properties of Metals* (Pergamon, New York, 1978).
[4]O. P. Sharma, Phys. Status Solidi B **86**, 483 (1978).
[5]F. Perrot, Phys. Status Solidi B **101**, 741 (1980).
[6]U. Fleck, H. Wonn, and P. Ziesche, Phys. Status Solidi A **61**, 447 (1980).
[7]Y. Yamada, Phys. Status Solidi B **102**, 629 (1980).
[8]M. Idrees, F. A. Khwaja, and M. S. K. Razmi, Phys. Status Solidi B **107**, 769 (1981).
[9]O. Jepsen, D. Glötzel, and A. R. Mackintosh, Phys. Rev. B **23**, 2684 (1981).
[10]A. H. MacDonald, J. M. Daams, S. H. Vosko, and D. D. Koelling, Phys. Rev. B **25**, 713 (1982).
[11]H. Eckardt, L. Fritsche, and J. Noffke, J. Phys. F **14**, 97 (1984).
[12]J. W. Davenport, Phys. Rev. B **29**, 2896 (1984).
[13]V. N. Antonov, Phys. Metals **6**, 931 (1985).
[14]C. S. Wang and J. Callaway, Comput. Phys. Commun. **14**, 327 (1978).
[15]J. Callaway and C. S. Wang, Phys. Rev. B **16**, 2095 (1977).
[16]C. S. Wang and J. Callaway, Phys. Rev. B **15**, 298 (1977).
[17]D. G. Laurent, C. S. Wang, and J. Callaway, Phys. Rev. B **17**, 455 (1978).
[18]D. G. Laurent, J. Callaway, and C. S. Wang, Phys. Rev. B **20**, 1134 (1979).
[19]D. G. Laurent, J. Callaway, J. L. Fry, and N. E. Brener, Phys. Rev. B **23**, 4977 (1981).
[20]P. Blaha and J. Callaway, Phys. Rev. B **32**, 7664 (1985).
[21]A. R. Jani, N. E. Brener, and J. Callaway, Phys. Rev. B **38**, 9425 (1988).
[22]G. S. Tripathi, N. E. Brener, and J. Callaway, Phys. Rev. B **38**, 10 454 (1988).
[23]H. Chen, N. E. Brener, and J. Callaway, Phys. Rev. B **40**, 1443 (1989).
[24]A. R. Jani, G. S. Tripathi, N. E. Brener, and J. Callaway, Phys. Rev. B **40**, 1593 (1989).
[25]R. Poirior, R. Kari, and I. G. Csizmadia, Phys. Sci. Data **34**, 9485 (1985).
[26]A. K. Rajagopal, S. P. Singhal, and J. Kimball (unpublished), as quoted by A. K. Rajagopal in *Advances in Chemical Physics,* edited by G. I. Prigogine and S. A. Rice (Wiley, New York, 1979), Vol. 41, p. 59.
[27]O. Jepsen and O. K. Andersen, Solid State Commun. **9**, 1763 (1971).
[28]G. Lehmann and M. Taut, Phys. Status Solidi **54**, 469 (1972).
[29]J. Rath and A. J. Freeman, Phys. Rev. B **11**, 2109 (1975).
[30]S. P. Singhal, Phys. Rev. **B12**, 564 (1975).
[31]J. Rath, C. S. Wang, R. A. Tawil, and J. Callaway, Phys. Rev. B **8**, 5139 (1973).
[32]C. S. Wang and J. Callaway, Phys. Rev. B **11**, 2417 (1975).
[33]D. G. Laurent and J. Callaway, Phys. Lett. **84A**, 499 (1981).
[34]J. G. Nelson, S. Kim, W. J. Gignac, and R. S. Williams, Phys. Rev. B **32**, 3465 (1985).
[35]H. Wern, R. Courths, G. Leschik, and S. Hüfner, Z. Phys. B **60**, 293 (1985).
[36]E. Sobczak, P. O. Nilsson, and J. Kanski, Phys. Rev. B **37**, 8150 (1988).
[37]S. C. Wu, C. K. C. Lok, J. Sokolov, J. Quinn, Y. S. Li, D. Tian, and F. Jona, J. Phys. Condens. Matter **1**, 4795 (1989).
[38]B. Kim, S. Hong, R. Liu, and D. Lynch, Phys. Rev. B **40**, 10 238 (1989).
[39]U. König, P. Weinberger, J. Redinger, H. Erschbaumer, and A. J. Freeman, Phys. Rev. B **39**, 7492 (1989).

[40]F. J. Himpsel, J. A. Knapp, and D. E. Eastman, Phys. Rev. B **19**, 2919 (1979); E. Eberhardt and E. W. Plummer, *ibid.* **21**, 3245 (1980).
[41]D. L. Martin, Phys. Rev. B **8**, 5357 (1973).
[42]G. Grimvall, Phys. Scr. **14**, 63 (1976).
[43]M. R. Halse, Phil. Trans. R. Soc. London, Ser. A **265**, 507 (1969).
[44]P. T. Coleridge and I. M. Templeton, Phys. Rev. B **25**, 7818 (1982).
[45]F. Biggs, L. B. Mendelsohn, and J. B. Mann, At. Data Nucl. Data Tables **16**, 201 (1975).
[46]D. G. Kanhere, R. M. Singru, and R. Harthoorn, Phys. Status Solidi B **105**, 715 (1981).
[47]B. K. Sharma, H. Singh, S. Perkkiö, T. Paakkari, and K. Mansikka, Phys. Status Solidi B **141**, 177 (1987).
[48]D. W. Lynch and W. R. Hunter, in *Handbook of Optical Constants of Solids,* edited by E. D. Palik (Academic, Orlando, 1985), p. 350.
[49]B. Dold and R. Mecke, Optik **22**, 435 (1965), as presented in Ref. 48.
[50]P. Winsemius, F. F. van Kampen, M. P. Lengkeek, and C. G. van Went, J. Phys. F **6**, 1583 (1976), as presented in Ref. 48.
[51]G. Leveque, C. G. Olson, and D. W. Lynch, Phys. Rev. B **27**, 4654 (1983).
[52]H. E. Bennett and J. M. Bennett, in *Optical Properties and Electronic Structure of Metals and Alloys,* edited by F. Abeles (North-Holland, Amsterdam, 1966), p. 181.
[53]K. A. Mills, Ph.D. thesis, University of California, 1979.